# EOS Validation of Aerosol and Water Vapor Profiles by Raman Lidar


## Abstract

We propose to use the aerosol extinction and backscattering profiles measured by two separate Raman lidar systems to validate the aerosol climatology models used by two EOS AM sensors, MODIS and MISR. The aerosol retrieval algorithms used by these EOS sensors operate by comparing measured radiances with tabulated radiances which have been computed for specific aerosol models. These aerosol models are based almost entirely on surface and/or column averaged measurements and so may not accurately represent the ambient aerosol properties. Therefore, to validate these EOS algorithms, we propose to evaluate the vertical variability of ambient aerosol properties using the aerosol backscattering and extinction profiles measured by the NASA/GSFC Scanning Raman Lidar (SRL), and the Dept. of Energy SGP (Southern Great Plains) CART (Cloud and Radiation Testbed) Raman Lidar.

In addition, we propose to use the aerosol and water vapor measurements acquired by both systems for directly validating the EOS instruments. Ground-based measurements of the vertical profiles of atmospheric water vapor and aerosols are required both for direct validation of these instruments as well as to understand the physical processes which affect the retrieval of aerosols and water vapor from these satellite platforms. Both Raman lidar systems directly measure profiles of water vapor mixing ratio, aerosol backscattering and extinction and can, therefore, also provide measurements of precipitable water vapor and aerosol optical thickness. We shall use the SRL aerosol data acquired during the TARFOX experiment at Wallops Island in July 1996 to assess the contribution made by different aerosol layers to the column integrated aerosol properties derived from the ground based sun/sky photometer measurements. We shall also use water vapor and aerosol measurements acquired by both lidars for similar studies during future experiments. Using the data from both lidar systems is a great asset for two reasons: 1) because it is a mobile instrument, the SRL will be able measure different types of aerosols at different locations, and 2) because it is designed for continuous, unattended operations, the SGP CART Raman lidar can acquire long term data sets required for validating EOS measurements over a long period of time.

## 1.0 Introduction

We propose to validate the aerosol and water vapor retrievals acquired by two EOS sensors, MODIS and MISR, using the aerosol and water vapor profiles measured by two Raman lidars. These studies are important for climate research since the Earth Observing System (EOS) will help support the U.S. Global Climate Research Program (USGCRP) by acquiring the data sets required to study global climate change. Included in these data sets are measurements of aerosols and water vapor. These atmospheric constituents play crucial roles in modulating the transfer of energy to and from the Earth. Water vapor is the most active infrared molecule in the atmosphere and so will play a major role in any global warming scenario associated with increased carbon dioxide (Ramanathan, 1988; Cess et al., 1990). Measurements of water vapor are important for characterizing atmospheric radiative properties because of the dominant role water vapor has in the computation of spectral effects throughout the longwave spectrum; uncertainties in the water vapor field dominate the spectral effects in the atmospheric window region (800-1200 $cm^{-1}$ or 8.3-12.5 μm) (DOE, 1990). The requirement for high accuracy in water vapor measurements is not limited to infrared radiance calculations; Fouquart et al. (1991) identified the calculation of water vapor absorption as one of the largest uncertainties in the computation of shortwave fluxes.

Atmospheric aerosols affect the earth's climate by scattering and absorbing solar radiation (direct effect) and by altering the scattering, absorption, lifetime, and extent of clouds (indirect effect). Recent modeling (Charlson et al, 1992; Kiehl and Briegleb, 1993, Box and Trautman, 1994) has indicated that the size of these aerosol effects is comparable (but opposite in sign) to that produced by the emission of greenhouse gases over the past century. Because of their short lifetime in the troposphere, aerosols have a large spatial and temporal variability in the troposphere so that it is very difficult to accurately assess their direct and indirect effects. Tropospheric aerosols pose the largest single uncertainty in computing the net radiative forcing due to anthropogenic changes in the chemical composition of the atmosphere (Hansen et al., 1993).

The MODIS sensor on the EOS AM platform will measure these key atmospheric constituents. The MODIS (Moderate-Resolution Imaging Spectroradiometer) Near-Infrared Total Precipitable Water Product will consist of column water vapor amounts over clear land areas, and above clouds over land and ocean (Gao and Kaufman, 1997). In addition, profiles of

water vapor will also be generated from the MODIS infrared radiances using techniques similar to those currently used for the High Resolution Infrared Radiation Sounder (HIRS) (Menzel and Gumley, 1995). For measurements over the oceans, the MODIS Aerosol Product will consist of aerosol optical thicknesses (AOT) and parameters which describe the size distribution; over land, this product will consist of AOT and aerosol type. The MISR (Multi-Angle Imaging SpectroRadiometer) Aerosol/Surface Product will contain a number of parameters including tropospheric aerosol optical thickness.

Extensive plans are underway for validating these aerosol and water vapor products. Since these aerosol and water vapor products represent for the most part column integrated aerosol and water vapor amounts, validation plans have focused primarily on acquiring similar measurements from ground based instruments. However, vertical profiles of both atmospheric water vapor and aerosols are required for evaluating these measurements, and perhaps more importantly, for understanding the physical and chemical processes which affect these retrievals of aerosols and water vapor from these satellite profiles. These measurements are needed to assess the effects of the vertical variability of aerosol optical and physical characteristics on the EOS MODIS and MISR retrieval algorithms. Moreover, simultaneous measurements of aerosols and water vapor profiles are required to understand the effects of water vapor on aerosol optical and physical properties. Such measurements are important because water vapor is a key meteorological factor which determines how aerosols affect radiative transfer. Significant changes in aerosol optical and physical properties associated with the uptake or release of water by hygroscopic sulfate aerosols have been measured extensively (Hanel, 1976; Charlson et al., 1984).

We propose to use profiles of aerosols and water vapor acquired by two separate Raman lidar systems to both evaluate these EOS measurements and to understand the processes which affect the retrievals from these EOS instruments. The NASA/Goddard Space Flight Center (GSFC) and Atmospheric Radiation Measurement (ARM) Southern Great Plains (SGP) Cloud and Radiation Testbed (CART) Raman Lidar both directly measure profiles of both aerosol backscattering and extinction and can, therefore, provide measurements of aerosol optical thickness to directly validate the EOS measurements. Similarly, both systems measure profiles of water vapor mixing ratio which can be used to derive precipitable water vapor.

We shall use the SRL measurements of aerosols acquired during the TARFOX experiment at Wallops Island in July 1996 to assess the contribution made by different aerosol layers to the column integrated aerosol properties derived from the ground based sun/sky photometer measurements. We shall also use these measurements, and other measurements acquired during future experiments, to ascertain the measurement capabilities and limitations of both the ground and aircraft based measurement techniques. The SRL is currently scheduled for deployment in tropical Atlantic to measure water vapor and aerosol profiles during the late summer and fall, 1998. We propose to use these profiles to evaluate the water vapor and aerosol retrievals acquired by MODIS. The SRL will also acquire similar measurements at the DOE SGP site in fall 1997 and in 1998 during a continuing series of water vapor and aerosol Intensive Operation Periods (IOPs). We shall use these measurements to evaluate and understand how the water vapor and aerosol measurement capabilities of the ARM SGP instrumentation, and in particular the CART Raman lidar, can be used for MODIS validation. We shall apply the procedures developed and demonstrated in the analyses of aerosol and water vapor data acquired by the SRL to analyze the aerosol extinction and backscattering profiles measured by the CART Raman Lidar. Because it is designed for continuous, unattended operations, the SGP CART Raman Lidar is well suited to provide the long term data sets required for validating the EOS MODIS and MISR measurements. We propose to use the aerosol and water vapor profiles measured by both systems for evaluating the MODIS aerosol and water vapor retrievals. In this proposal, we shall first describe these lidar systems, discuss their measurement capabilities, the importance of these measurements for EOS instruments, and outline our proposed research using these measurements for EOS Validation studies.

## 2.0 NASA/GSFC Scanning Raman Lidar

### 2.1 Water Vapor Measurements

The GSFC Scanning Raman Lidar employs two different lasers depending on whether data are acquired at nighttime or daytime. For nighttime operations, this system uses an XeF excimer

laser to transmit pulses of light at 351 nm. The laser operates at 400 Hz with 30 millijoules per pulse giving an average power of 12 W. Light backscattered by molecules and aerosols at the laser wavelength as well as Raman scattered light from water vapor (402 nm), nitrogen (383 nm), and oxygen (372 nm) molecules is collected by a 0.76 m, F5.2, variable field-of-view (.5 - 3.0 milliradians) Dall-Kirkham telescope which is mounted horizontally on a 3.7m optical table. The telescope is aligned with a large (1.2m x .8m) flat mirror which is also mounted on the optical table. During operations, the optical table slides through an opening in the back of the trailer deploying the scan mirror which has a 180 degree horizon to horizon scan capability. Using the motorized scan mirror, atmospheric profiles can be acquired at any angle in a single plane perpendicular to the trailer or continuously scanned from horizon to horizon.

The ability of the GSFC lidar to scan to the horizon is important for studying tropospheric aerosols. Most lidar systems have a "semi-blind" region near the lidar where the laser beam is not fully within the field of view of the receiving telescope. While this overlap region can normally be characterized sufficiently to compute the aerosol scattering ratio and the water vapor mixing ratio, parameters such as aerosol extinction obtained using data from a single channel can not be computed in this region. Therefore, this ability to acquire data at nearly horizontal angles permits this system to measure aerosol extinction close to the surface. This ability to point nearly horizontally also permits the lidar to acquire coincident measurements of aerosols and water vapor with co-located tower based instrumentation.

Two channels, operating in the photon counting mode, are employed for each wavelength in order to measure signals throughout the troposphere and lower stratosphere. In normal operation, data are recorded as one-minute profiles corresponding to the accumulation of signals from about 23000 laser shots. The photon counting data have a range resolution of 75 meters. Unless otherwise specified, the data discussed in this proposal were acquired at night to minimize the interference from background skylight that interferes with the detection of the Raman signals, which are about three orders of magnitude weaker than the signal due to Rayleigh and Mie backscatter from molecules and aerosols. The entire lidar system is contained in two,

environmentally controlled trailers; one trailer houses the system described above, while the second contains computers for data acquisition and analysis and the operating personnel. Several analysis programs operate in real-time to monitor system performance and to provide real-time images of the evolution of both aerosols and water vapor.

To facilitate daytime measurements, the SRL has recently been upgraded by adding a tripled Nd:YAG laser, narrowband interference filters, and a dual (narrow and wide) field of view optics design. This laser, which transmits light at 355 nm, operates at 30 Hz with 300 millijoule pulses giving an average power of about 9 W. The laser beam divergence is reduced to below 0.2 mrad by means of a x3 beam expander; this low divergence permits the use of a narrow (0.25 mrad) field of view in addition to the wide (2.0 mrad) field of view. The narrow field of view, coupled with the use of narrowband (~0.2-0.3 nm bandpass) filters, reduces the background skylight and, therefore, increases the signal/noise ratio during the daytime operations. During daytime operations, the light backscattered at this wavelength is detected as well as the Raman returns from water vapor (408 nm), nitrogen (387 nm), and oxygen (376 nm) molecules.

The SRL has been used extensively to measure atmospheric water vapor (Soden et al., 1994, Han et al., 1994, Wang et al., 1995, Ferrare et al., 1995). The water vapor mixing ratio, which is defined as the mass of water vapor divided by the mass of dry air, is derived from the ratio of Raman water vapor to Raman nitrogen signals. The lidar water vapor profiles are then used in conjunction with temperature profiles measured by radiosondes as well as derived from coincident downwelling radiances measured by the AERI instrument (Smith et al., 1995) to compute relative humidity profiles. Precipitable water is derived by integrating the water vapor mixing ratio profile with pressure. Details of these procedures are discussed by Ferrare et al. (1992, 1993) and Whiteman et al. (1992).

The SRL water vapor calibration is normally obtained by comparing the lidar water vapor ratios with water vapor mixing ratio profiles measured by coincident radiosondes (Ferrare et al., 1995). This calibration constant has been found to vary depending on the type of radiosonde used for comparison. Figure 1 shows the water vapor calibration constant obtained from several field experiments including the RCS IOP held at the SGP site in 1994 and, most recently, at the DOE SGP site during the Water Vapor IOP in September, 1996. The lidar water vapor calibration constant varied by less than 5% over a five-year period when calibrated using Vaisala radiosondes

and 7% when calibrated using AIR/VIZ radiosondes. There is about a 5-7% difference in the calibration constant depending on the type of radiosonde sensor used in the comparison. The Vaisala sondes use a capacitive element to measure water vapor while the AIR/VIZ sondes use a carbon hygristor humidity sensing element. These differences emphasize the need for using other measurements in addition to radiosonde measurements to accurately evaluate satellite estimates of water vapor profiles.

The NASA/Goddard Space Flight Center Scanning Raman Lidar (SRL) was used during recent field experiments to evaluate water vapor measurements acquired by other sensors. The SRL acquired 67 hours of data were acquired over 16 nights of operation during the CAMEX-2 (Convection and Moisture-2) and LASE (Laser Atmospheric Sensing Experiment) held at Wallops Island, Virginia in August and September, 1995. Water vapor profiles derived from SRL data acquired during the CAMEX2/LASE/WMO experiments were compared with water vapor profiles acquired by: Vaisala and VIZ radiosondes, the LASE water vapor DIAL (differential absorption lidar) lidar flown on the NASA ER-2 (Browell, 1995), and GE 1011 chilled mirror dew point hygrometers flown on two additional aircraft (a Lear jet and a C-130). In addition, by pointing nearly horizontally, the lidar water vapor measurements were compared with those measured by a hygrometer mounted on the top of a building 3.2 km away. Bias and root-mean-square differences between the lidar water vapor mixing ratio profiles and those from the instruments listed above were found to be less than 5-10%. Figure 2 shows comparisons of the SRL water vapor measurements and those acquired by aircraft dew point hygrometers and by the LASE lidar.

During the Water Vapor Intensive Operations Period (IOP) held during September 1996 at the DOE ARM SGP site near Lamont, Oklahoma, the SRL measured water vapor during both daytime and nighttime operations in order to help characterize the water vapor in the lowest kilometer of the atmosphere and to develop an accurate calibration of the CART Raman lidar without relying on radiosondes. Several different instruments participated including Raman lidars, radiosondes, microwave radiometers, dew point hygrometers, GPS (Global Positioning System), and surface and tower mounted hygrometers. The scanning ability of the SRL facilitated comparisons with the tower and surface sensors; in addition, by integrating the SRL data, precipitable water vapor (PWV) amounts were also computed and used to assess PWV

measurements made by other systems. Figure 3 shows how the SRL water vapor measurements can be compared with other water vapor measurements: 1) profile comparisons with radiosondes, chilled mirror dewpoint hygrometer, and the CART Raman Lidar, 2) point measurements using scan data with tower based measurements, and 3) PWV comparisons with microwave radiometers. During the Water Vapor IOP, the daytime water vapor measurement capability was also demonstrated. Figure 4 shows a color image showing water vapor measurements acquired during both daytime and nighttime operations on September 29, 1996; figure 4 also shows a comparison of the water vapor profile acquired on the afternoon of September 29 along with a radiosonde profile.

### 2.2 Aerosol Measurements

Although primarily designed to measure profiles of water vapor mixing ratio, this lidar system has also been used extensively to measure aerosol profiles. The aerosol scattering ratio, which is defined as the ratio of the total (aerosol+molecular) scattering to molecular scattering, is computed directly from the lidar data. Molecular backscattering is measured using the Raman nitrogen return while the combined aerosol+molecular backscattering is measured using the return signal at the laser wavelength. The aerosol volume backscatter cross section is then computed from the scattering ratio and the molecular backscattering cross section which is derived from the coincident radiosonde pressure and temperature profiles. Cloud base altitudes are easily determined from the aerosol scattering ratio profiles. Details of these aerosol algorithms are given by Ferrare et al. (1992) and Whiteman et al. (1992).

Unlike most lidars which measure only the signal directly backscattered by molecules and aerosols, Raman lidar is also used to simultaneously and directly measure the aerosol volume extinction cross section since aerosol extinction (not backscattering) affects these Raman signals (Ansmann et al., 1990). The total extinction, due to both scattering and absorption by molecules and aerosols, is found from the derivative of the logarithm of the nitrogen Raman return signal. Aerosol extinction is then found by subtracting molecular extinction which is computed using coincident radiosonde density measurements. Using the Raman signal to compute aerosol extinction avoids having to assume some generally unknown relationship between aerosol

backscattering and extinction which otherwise must be done to invert the return signal at the laser wavelength to compute aerosol extinction (Klett, 1981).

The Raman technique measures the sum of the aerosol extinction coefficients at two wavelengths, the outgoing laser wavelength and the return Raman nitrogen (and/or oxygen) wavelength. If the wavelength dependence of aerosol extinction is known, the aerosol extinction cross section can be found at either of these two wavelengths. The wavelength dependence $\lambda^{-k}$ between the laser wavelength of 355 nm and the Raman nitrogen return signal at 387 nm is normally assumed to be unity (k=1) (Ansmann et al., 1990) but can vary depending on the size and composition of aerosols. Aerosol optical thicknesses measured between 340 nm and 440 nm by a Cimel sun photometer (Holben et al., 1995; Remer et al., 1997) co-located with the SRL at Wallops Is. and at the DOE SGP site near Lamont, OK have shown k varies between 0 and 2. The error in the derived aerosol extinction at 355 nm using the Raman nitrogen signal is +/-10% if k varies between 0 and 2 when an assumed value of k=1 is used. This error is significantly reduced if the wavelength dependence of aerosol extinction is known. We propose to estimate this wavelength dependence using sun photometer measurements of aerosol optical thickness as we have done in these previous experiments. In addition, the Raman technique also requires profiles of atmospheric density which can be computed from pressure and temperature profiles measured by radiosondes launched at the SGP site and/or from profiles derived from the AERI instrument (Smith et al., 1995).

Measurements of the aerosol optical thickness can be derived by integrating the aerosol extinction profiles measured by Raman lidar. Figure 5 shows a comparison of the aerosol optical thickness measured by the NASA/GSFC Raman lidar and a CIMEL sun photometer during 9 days of operations during TARFOX (Tropospheric Aerosol Radiative Forcing Observational Experiment) held at Wallops Is. during July, 1996. This sun photometer is the same model as those which comprise the AERONET network to be used to validate the MODIS aerosol optical thickness measurements. Figure 6 shows a direct comparison of the aerosol optical thicknesses measured by the two systems for cloud free conditions; the aerosol optical thicknesses measured by both techniques agree to within about 5%. The smaller number of sun photometer measurements on several days shown in figure 5 was due primarily to the inability of the sun photometer to measure AOT in the presence of clouds. Since Raman lidar measurements of

aerosol optical thickness can occur during both during both daytime and nighttime, as well as in the presence of clouds, Raman lidar can measure aerosol optical thickness during times when the sun photometer is unable to provide data.

The Raman lidar aerosol profiles can be used in conjunction with other measurements to estimate the physical characteristics of aerosols and to determine how these characteristics vary with altitude. Ferrare (1997a) describes a technique to estimate the aerosol hygroscopic growth factor, real refractive index, and single scattering albedo using the Raman lidar aerosol backscattering and extinction profiles along with airborne measurements of the aerosol size distribution. In this technique, profiles of aerosol extinction and backscattering are computed from Mie theory using the measured aerosol size distributions as functions of these aerosol parameters. These computed profiles are then compared in an iterative fashion with the corresponding profiles measured by Raman lidar to determine the appropriate parameters. These comparisons make use of both aerosol backscattering and extinction profiles.

This technique was developed using data acquired at the SGP site during April, 1994. Figure 7 shows images of water vapor mixing ratio, relative humidity, aerosol backscattering and aerosol extinction derived from the GSFC Raman Lidar data acquired on April 21, 1994 at the SGP site during the RCS IOP. Note that both the water vapor and aerosol images show that there is an elevated layer of water vapor and aerosols with highest concentrations of water vapor and aerosols just above 4 km. In addition, there is an increase in both aerosol backscattering and extinction throughout the lowest 1.5 km beginning between 4-5 UT. There is a more pronounced aerosol feature within the lowest 400 meters which begins to appear around 0700 UT. Figure 8 shows representative size distributions for aerosols in the lower altitudes of 0.63 km (ascent) and 0.7 km (descent) while distributions for the upper layers are represented at altitudes at 4.6 km (ascent) and 4.5 km (descent). Figure 8 shows that there was an increase in the number of accumulation mode particles with radii near 0.1μm in the lower layer. In addition, the number of the particles in the lower layer increased with time between aircraft ascent and descent. Figure 9 shows profiles of the real refractive index and single scattering albedo required to derive the aerosol extinction and backscattering profiles which most closely match those simultaneously measured by the Raman lidar; these derived and measured aerosol extinction and backscattering

profiles are also shown in figure 9. Note that the aerosol extinction/backscattering ratio measured by the lidar and derived from the calculations varied with both time and altitude below 2 km.

This example shows how the Raman lidar measurements of both aerosol backscattering and extinction, when combined with measurements of the aerosol size distribution, can be used to estimate the aerosol real refractive index and single scattering albedo (i.e. aerosol absorption). Alternatively, these lidar profiles can be used in column closure studies to evaluate the aerosol extinction and scattering profiles derived from measurements of aerosol size distribution and composition from aircraft and surface sensors (Quinn et al., 1996). Raman lidar measurements of aerosol profiles acquired during the TARFOX experiment are being used in this capacity.

## 3.0 SGP CART Raman Lidar

The examples given above have shown how aerosol backscattering and extinction profiles measured by the NASA/GSFC Raman lidar have been used to derive aerosol physical properties and investigate the relative humidity dependence of aerosol extinction. In addition to the data acquired by the SRL system, we propose to also use data acquired by a similar Raman Lidar system: the SGP CART Raman Lidar (Goldsmith et al., 1996). This Raman lidar system is unique in that it is designed specifically for continuous, unattended operations. In April 1997, this system began routine 24 hour/day operations for profile measurements of both water vapor and aerosols. This lidar measures Raman scattering from water vapor and nitrogen as well as the scattering from molecules and aerosols at the laser wavelength. Water vapor and relative humidity profiles are derived in the same manner as those derived from the GSFC Raman Lidar data.

The ability of the CART Raman Lidar to provide water vapor profiles was demonstrated during the Water Vapor IOP held in September, 1996. Water vapor profiles measured by the CART Raman Lidar were compared with those measured by radiosondes, the GSFC Raman Lidar, and chilled mirror dew point hygrometers flown on a tethersonde. Precipitable water vapor amounts were compared with those measured by the SGP microwave radiometer and GPS; water vapor measurements made at an altitude of 60 meters were compared with those measured on an instrumented tower. Figure 10 shows a comparison of the CART Raman Lidar water vapor amounts, when calibrated using the SGP microwave radiometer, with those measured by the other

sensors (Turner and Goldsmith, 1997). With the exceptions of the Vaisala 62 series radiosonde and the tethersonde chilled mirror, the CART Raman Lidar water vapor measurements generally agree within 5% with those derived from the other sensors.

Aerosol scattering ratio profiles have also been computed from the CART Raman Lidar data. An example of these data are shown in figure 11 which shows aerosol scattering ratio measured by the SGP Raman Lidar on September 23, 1996 during the Water Vapor IOP. Figure 11 also shows the relative humidity during this same period. These relative humidity profiles were computed using water vapor mixing ratio profiles measured by the CART Raman Lidar and temperature profiles derived from the AERI radiances (Smith et al., 1995). Both the CART Raman Lidar water vapor mixing ratio profiles and AERI temperature profiles have a temporal resolution of 10 minutes. The white regions shown in the aerosol scattering ratio image are due to the presence of clouds. Note the region of hygroscopic aerosols as indicated by the correspondence between the region of high aerosol scattering ratio (shown by yellow and red regions) and high relative humidities (shown by violet and white regions) for altitudes between 0.8-1.2 km for the period between 02:00-03:30 UT.

With support from the Dept. of Energy, we are currently working toward the development of algorithms for computing aerosol backscattering and extinction coefficients using the CART Raman Lidar data. While these algorithms are based on those methods developed for the SRL, we are working on the resolution of system issues specifically related to the CART Raman Lidar. We are using the data acquired by both lidar systems during the Water Vapor IOP experiment for the development and evaluation of these algorithms.

## 4.0 EOS Measurements

### 4.1 Aerosol Measurements

The MODIS instrument flown on the EOS satellite will be used to measure aerosol optical thickness over most of the globe on a daily basis. In addition, the relative contribution of aerosol scattering due to both the accumulation (particle diameters between 0.05 to 1.0 μm) and coarse

(particle diameters > 1.0 μm) particle modes will be derived over the oceans. The MISR instrument flown on EOS will measure aerosol optical thickness over the globe.

The algorithms used to derive aerosol optical thicknesses from the MODIS and MISR measurements of spectral radiances are somewhat similar. In these retrievals, a lookup table of spectral radiances is created from forward radiative transfer calculations using various aerosol and surface parameters. The aerosol parameters used to compute these aerosol radiances include the particle size distribution, the refractive index, and the single scattering albedo. For the retrieval of aerosol optical thickness over water, the measured spectral radiances are then compared with the pre-computed values in the lookup table until the best fit is obtained; the aerosol optical thickness corresponding to the aerosol parameters used to compute these lookup radiances is the derived value. The aerosol optical thickness retrievals over land use radiances measured over dark vegetation where the surface reflectance is low. The aerosol models used in the radiative transfer computations use climatologies of aerosol models specified by d'Almeida et al. (1991) and Shettle and Fenn (1979). These models specify aerosol characteristics for particular aerosol types including: desert aerosols (d'Almeida, 1987; Shettle, 1984), maritime aerosols (Hoppel et al., 1990), or aerosols resulting from biomass burning in tropical regions (Kaufman et al., 1992).

The aerosol climatologies used in these aerosol models are based almost entirely on surface measurements and, therefore, may not represent the whole atmospheric column or the properties of the ambient aerosol (Kaufman and Tanre, 1997). Additional measurements from ground based sun/sky sun photometers (Kaufman et al., 1994; Holben et al., 1995) are used to supplement these climatologies with ambient measurements integrated throughout the entire atmospheric column (Kaufman and Holben, 1996; Remer et al., 1997). However, these additional sun photometer measurements can not measure the vertical distribution of aerosols nor can they measure how the aerosol optical and physical characteristics vary with altitude and relative humidity. This is a major limitation since both in-situ and remote sensing measurements have shown that aerosol properties often vary significantly with altitude. In-situ measurements of aerosols collected near Bermuda show that the size distributions at high altitudes differed from those at low altitudes (Horvath et al., 1990). Remer et al. (1997) examined aerosol size distributions measured by airborne in-situ instrumentation and those derived from sun photometer almucantar measurements acquired during the SCAR-A experiment conducted at Wallops Island,

VA during the summer of 1993. The airborne in-situ data showed considerable variations with altitude of both the accumulation and coarse particle mode size distributions. Ferrare (1997b) used a combination of aerosol extinction and backscattering profiles measured by the GSFC Raman lidar and aerosol size distributions measured by a PCASP optical particle counter flown on the University of North Dakota Citation aircraft to show that the particle real refractive index and single scattering albedo varied with altitude (recall figure 9). Since the particle size distribution and composition often vary with altitude, the variation of aerosol scattering with relative humidity can also be expected to vary with altitude. Satellite observations have shown that aerosols produced by large forest fires in northwest Canada are transported thousands of kilometers from the source region and have been observed over the eastern U.S. and the Atlantic Ocean (Ferrare et al., 1990). Such long range transport implies that aerosols observed over the eastern U.S. often reside in elevated layers above the convective boundary layer and can not, therefore, be attributed to the sulfate aerosols produced locally by either natural or anthropogenic sources.

Information regarding the vertical distribution of aerosol properties can also help in the understanding of the behavior of the various modes observed in the retrieved aerosol size distributions. Tropospheric aerosol size distributions derived from sun photometer solar almucantar data acquired over the eastern U.S. during the SCAR-A experiment in 1993 displayed three modes: sulfate particles in the accumulation mode ($r < 0.3$ um); a slightly larger maritime salt particle mode ($0.8<r<2.5$ um); and a coarse particle mode ($r>2.5$ um) (Kaufman and Holben, 1996, Remer et al., 1997). The average accumulation mode particle size was found to increase with aerosol optical thickness; this growth was attributed to the aging of particles, growth in the in-cloud processes (Hoppel et al., 1990), and hygroscopic growth associated with high relative humidity. Similar growth was not observed for smoke aerosols. Significant changes in aerosol optical and physical properties associated with the uptake or release of water by hygroscopic sulfate aerosols have been measured extensively (Hanel, 1976; Charlson et al., 1984). Both lidar measurements during daytime (Dupont et al., 1994) and nighttime (Ferrare et al., 1993,1995) and airborne integrating nephelometer measurements (Kaufman et al., 1986) have shown aerosol scattering is often highly correlated with relative humidity (recall figure 11). The single most important parameter in assessing the direct aerosol forcing is relative humidity, due to the increase in aerosol mass associated with water uptake (Pilinis et al., 1995). This growth behavior could be

investigated further if vertical profiles of both aerosols and water vapor were available. Such measurements could determine if variations in optical thickness were associated with either variations in aerosols throughout the mixed layer, variations in aerosol optical properties near the top of the mixed layer associated with relative humidity effects, or due to the presence of elevated aerosol layers associated with long range aerosol transport.

Profiles of aerosol optical (and physical) properties can be acquired from aircraft platforms. Measurements of aerosol properties will in fact occur during MODIS-specific Validation Field Missions. However, aircraft aerosol measurements can be problematic. Aircraft in-situ measurements often subject the aerosols to changes in relative humidity between the atmosphere and the instrument (Baumgardner and Huebert, 1993). The aerosol collection efficiency depends on size and, therefore, may not correctly represent all sizes of particles correctly (Huebert et al., 1990). More importantly, the cost of these aircraft measurements prohibits their use for routine day-to-day operations. Thus, other methods must be used to provide routine measurements of aerosol extinction profiles for studying radiative transfer on a continuous basis.

Lidar has proven to be an effective instrument for obtaining high resolution profiles of atmospheric aerosols. The MicroPulse Lidar (MPL) has been proposed as one potential method for measuring aerosol extinction profiles (Spinhirne et al., 1996). One potential method is to use the aerosol optical thickness measurements from the MFRSR and/or CIMEL sun photometer and to distribute this aerosol amount using aerosol backscattering profiles from the MPL; however, the need for coincident measurements of aerosol optical thickness from the MFRSR restricts this method to daytime, cloud-free periods. Spinhirne et al. (1996) also discuss the potential for using MPL data to directly derive aerosol extinction. However, such methods which attempt to make quantitative measurements of aerosol optical properties using a lidar system which measures only aerosol backscatter requires accurate system calibration and some assumptions regarding aerosol parameters (Klett, 1981; Fernald, 1984). These restrictions are necessary since these systems attempt to derive two aerosol parameters (backscatter and extinction) with only one measured signal so that some relationship between these two parameters must be assumed.

The ability of a Raman lidar to simultaneously and directly measure profiles of both aerosol backscattering and extinction without requiring these assumptions is a great advantage.

Aerosol extinction and backscattering profiles measured by the GSFC Raman Lidar during the RCS IOP at the SGP site in April, 1994 have shown that the relationship between aerosol extinction and backscattering often varies with both time and altitude (recall figure 7). These variations in the aerosol extinction/backscattering ratio are indicative of changes in the aerosol physical characteristics (size, composition, and/or shape). Thus, the profiles of both aerosol extinction and backscattering derived from Raman lidar measurements can be used to remotely monitor the variation in aerosol characteristics within the atmospheric column.

### 4.2 Water Vapor Measurements

MODIS will also be used to provide measurements of column water vapor amounts over the globe. These retrievals are based on measuring the absorption of solar radiation in the 940 nm water vapor absorption band. These water vapor retrievals are expected to be validated with a variety of sensors including: microwave radiometers, radiosondes, and sun photometers. As discussed in section 2.1, Raman lidar has also been used to measure precipitable water and could, therefore, also provide water vapor amounts to validate these MODIS column water vapor amounts.

MODIS will also be used to provide profiles of temperature and water vapor. These retrievals will be performed using similar retrieval algorithms as are used for the HIRS (High Resolution Infrared Radiation Sounder) which is currently flown on the polar orbiting NOAA TIROS Operational Vertical Sounder (TOVS). The algorithms for the MODIS retrievals will be adapted from those used for the operational TOVS and GOES sensors and will be modified to utilize the greatly increased spatial resolution on MODIS (Menzel and Gumley, 1995).

Validation of the water vapor profiles retrieved from the MODIS measurements will require coincident measurements of water vapor profiles. While radiosondes could provide such measurements, accurate evaluation of these MODIS profiles would be difficult to achieve using these measurements. Comparisons of radiosonde water vapor profiles with those acquired by the GSFC Raman lidar have revealed differences of 5-8% between various radiosonde humidity sensors (Ferrare et al., 1995). Moreover, comparisons of water vapor profiles acquired during the Water Vapor IOP held at the DOE SGP site in September, 1996 revealed that the water vapor

measurements from a single type of radiosonde sensor (Vaisala-H humicap) manufactured at different times can vary by 10% (Melfi et al, 1997; Turner and Goldsmith, 1997; Liljegren and Lesht, 1997).

As in the case of aerosol profiles discussed above, water vapor profiles required to calibrate these MODIS water vapor retrievals could also be obtained from aircraft measurements. Such measurements could be obtained from either in-situ sensors such as dew point and frost point hygrometers, or from remote sensors such as the LASE lidar system (Browell et al., 1997). However, these airborne validation studies would again be limited to specific field experiments and, therefore, would not be able to provide routine water vapor measurements required for these validation studies.

## 5.0 Objectives and Methodology

We propose to use the Raman lidar measurements of aerosols and water vapor acquired by two separate systems, the NASA/GSFC Scanning Raman Lidar, and the DOE SGP CART Raman Lidar, for EOS Validation Studies. These studies will be comprised of the following activities:

**1) Use the vertical profiles of aerosol backscattering and extinction collected by the GSFC Raman Lidar during the TARFOX experiment for EOS validation studies by assessing the vertical distribution of aerosols and how these distributions compare with those used for MODIS and MISR algorithms.**

These profiles will be used to measure the boundary layer thickness and locate the presence of elevated haze layers. These lidar measurements will also be used to assess whether changes in aerosol optical thickness observed by the sun photometers are due to 1) long range transport of aerosols in elevated layers above the convective boundary layer (CBL), and/or 2) increases in aerosol concentrations throughout the CBL. The lidar profiles of aerosol extinction will be integrated to obtain aerosol optical thickness; this will permit direct comparisons with the sun photometer instruments and will help ascertain the sun photometer calibration. The lidar backscatter measurements will also be used to identify the presence of thin clouds which may otherwise escape detection by the sun photometer optical thickness detection schemes. Lidar

measurements of the altitude distributions of aerosols will be used to convert the aerosol size distributions derived from sun photometer solar almucantar measurements into total volume size distributions following the procedure described by Remer et al. (1995b).

**2) Use the measurements of aerosol extinction and backscattering profiles collected by the SGP CART Raman Lidar to investigate, over an extended period of time, how the aerosol properties over the SGP EOS Validation Site vary with altitude and time.**

The potential for the SGP CART Raman Lidar to provide continuous, 24 hour/day measurements of both aerosol backscattering and extinction would make this an ideal instrument to provide EOS Validation data. Such measurements could be used to provide direct validation of aerosol optical thickness as well as to investigate the applicability of the aerosol properties and vertical distributions used to construct the aerosol models. These lidar data, when combined with the Cimel sun photometer data located at the SGP site, would provide valuable long term data to determine the aerosol variability within the atmospheric column measured by both MODIS and MISR as well as the ground based sun photometers. This variability could be monitored using the lidar remote measurements of the aerosol extinction/backscattering ratio.

**3) Use the aerosol and water vapor measurements acquired by the NASA/GSFC Scanning Raman Lidar (SRL) during future experiments to evaluate both the MODIS and MISR aerosol and water vapor measurements as well as the ground based instruments used to provide validation data for these EOS instruments.**

The SRL is currently scheduled for deployment in CAMEX-3 (Convection and Moisture Experiment-3) to the tropical Atlantic to measure water vapor and aerosol profiles during the late summer and fall, 1998. We propose to use these profiles to measure precipitable water vapor and aerosol optical thickness to evaluate the corresponding values derived from MODIS and MISR. We shall also use the lidar water vapor profiles to evaluate the water vapor profiles derived from MODIS.

The SRL is also scheduled for deployment to the SGP site in the fall of 1997 to participate in the Water vapor and Aerosol IOPs. We propose to use the water vapor, aerosol extinction and backscattering profiles collected during this experiment to evaluate the performance of the SGP CART Raman Lidar. This evaluation is of particular importance in the case of aerosol profiles for the following reasons: 1) the algorithms used to derive profiles of aerosol backscattering and

extinction from the SGP CART Raman Lidar are still under development and, therefore, will require validation, and 2) unlike in the case of water vapor, there will not be a significant amount of additional information to evaluate the aerosol profiles measured by the SGP CART Lidar.

## 10.0 References


Ansmann, A., M. Riebesell, and C. Weitkamp, 1990: Measurement of atmospheric aerosol extinction profiles with a Raman lidar, *Optics Letters*, **15**, 746-748.

Baumgardner, D. and B. Huebert, 1993: The airborne aerosol inlet workshop: Meeting report, *J. Aerosol Sci.*, **24**, No. 6, 835-846.

Box, M.A., and T. Trautman, 1994: Computation of anthropogenic sulphate aerosol forcing using radiative perturbation theory, *Tellus*, **46B**, 33-39.

Browell, E.V., 1995: Airborne Lidar Measurements, *Rev. of Laser Engineering*, **23**, No. 2, 135-141.

Browell, E.V., S. Ismail, W.M. Hall, A.S. Moore, Jr., S.A. Kool, V.G. Brackett, M.B. Clayton, J.D.W. Barrick, F.J. Schmidlin, N.S. Higdon, S.H. Melfi, and D. N. Whiteman, 1997: LASE Validation Experiment, in Advances in Atmospheric Remote Sensing with Lidar, Springer-Verlag, Berlin, 289-295.

Cess, R.D., G.L. Potter, J.P. Blanchet, G.J. Boer, A.D. Del Genio, M. Deque, V. Dymnikov, V. Galin, W.L. Gates, S.J. Ghan, J.T. Kiehl, A.A. Lacis, H. Le Treut, Z.-X. Li, X.-Z. Liang, B.J. McAvaney, V.P. Meleshko, J.F.B. Mitchell, J.J. Moncrette, D.A. Randal, L. Rikus, E. Roeckner, J.F. Royer, U. Schlese, D.A. Sheinin, A. Slingo, A.P. Sokolov, K.E. Taylor, W.M. Washington, R.T. Wetherald, I. Yagai, and M.H. Zhang, 1990: Intercomparison and Interpretation of Climate Feedback Processes in 19 Atmospheric General Circulation Models, *J. Geophys. Res.*, **95**, 16601-16615.

Charlson, R.J., D.S. Covert, and T.V. Larson, 1984: Observation of the effect of humidity on light scattering by aerosols, in Hygroscopic Aerosols, L. Ruhnke and A. Deepak, (eds.), A. Deepak Publishing, 35-44.

Charlson, R.J., S.E. Schwartz, J.M. Hales, R.D. Cess, J.A. Coakley, Jr., J.E. Hansen, D.J. Hofmann, 1992: Climate forcing by anthropogenic aerosols, *Science*, **255**, 423-430.

DOE, 1990: *Atmospheric Radiation Measurement Program Plan*, U.S. Department of Energy, DOE/ER-0441, Washington, D.C.

d'Almeida, G.A., 1987: On the variability of desert aerosol radiative characteristics, *J. Geophys. Res.*, **93**, 3017-3026.

d'Almeida, G.A., P. Koepke, and E.P. Shettle, 1991: Atmospheric Aerosols: Global Climatology and Radiative Characteristics, A. Deepak Publishing, Hampton, VA, 559 pp.

Dupont, E., J. Pelon, and C. Flamant, 1994: Study of the moist convective boundary-layer structure by backscattering lidar, *Boundary Layer Meteor.*, **69**, 1-25.

Fernald, F.G., 1984: Analysis of atmospheric lidar observations: some comments, *Appl. Opt.*, **23**, 652-653.

Ferrare, R.A., R.S. Fraser, and Y.J. Kaufman, 1990: Satellite Measurements of Large Scale Air Pollution - Measurements of Forest Fire Smoke, *J. Geophys. Res.*, **95**, D7, 9911-9925.

Ferrare, R.A., S.H. Melfi, D.N. Whiteman, and K.D. Evans, 1992: Raman lidar measurements of Pinatubo aerosols over southeastern Kansas during November-December 1991, *Geophys. Res. Letters*, **19**, No. 15, 1599-1602.

Ferrare, R.A, S.H. Melfi, D.N. Whiteman, and K.D. Evans, 1993: Coincident Measurements of Atmospheric Aerosol Properties and Water Vapor by a Scanning Raman Lidar, in Optical Remote Sensing of the Atmosphere Technical Digest, 1993 (Optical Society of America, Washington, D.C., 1993), Vol. 5, 11-14.

Ferrare, R.A., S.H. Melfi, D.N. Whiteman, K.D. Evans, F.J. Schmidlin and D.O'C. Starr, 1995: "A Comparison of Water Vapor Measurements made by Raman Lidar and Radiosondes," *J. Atmos. Ocean Tech.*, **12**, 1177-1195.

Ferrare, R.A., 1997a: The Applicability of a Scanning Raman Lidar for Measurements of Aerosols and Water Vapor, Ph.D. Thesis, University of Maryland College Park, 170 pp.

Ferrare, R.A., S.H. Melfi, D. Whiteman, K.D. Evans, G. Schwemmer, Y. Kaufman, R. Ellingson, 1997b: Raman Lidar and Sun Photometer Measurements of Aerosols and Water Vapor, in Advances in Atmospheric Remote Sensing with Lidar, A. Ansmann, R. Neuber, P. Rairoux, U. Wandinger, eds., Springer-Verlag, Berlin, p. 23-26.

Fouquart, Y., B. Bonnel, and V. Ramaswamy, 1991: Intercomparing shortwave radiation codes for climate studies, *J. Geophys. Res.*, **96**, No. 5, 8955-8968.

Gao, B.C. and Y.J. Kaufman, 1997: The MODIS Near-IR Water Vapor Algorithm, EOS Algorithm Technical Background Document, ATBD-MOD-03.

Goldsmith, J.E.M., F.H. Blair, and S.E. Bisson, 1996: Implementation of Raman Lidar for Profiling of Atmospheric Water Vapor and Aerosols at the Southern Great Plains (SGP) Cloud and Radiation Testbed (CART) Site ., Proceedings of the Fifth Atmospheric Radiation Measurement Program Science Team Meeting, San Antonio, TX.

Han, Y., J.B. Snider, E.R. Westwater, S.H. Melfi, and R.A. Ferrare, 1994: Observations of water vapor by ground-based microwave radiometers and Raman lidar, *JGR*, **99**, 18695-18702.

Hanel, G., 1976: An attempt to interpret the humidity dependencies of the aerosol extinction and scattering coefficients, *Atmos. Environ.*, **15**, 403-406.

Hansen, J., W. Rossow, and I. Fung, 1993: Long-term monitoring of global climate forcings and feedbacks, Proc. Workshop, GISS, 3-4 February 1992, NASA Conference Publication 3234.

Holben, B.N., T.F. Eck, I.Slutsker, D. Tanre, J.P. Buis, A. Setzer, E. Vermote, J.A. Reagan, and Y.J. Kaufman, 1995: Multi-band automatic sun and sky scanning radiometer for measurement of aerosols, Proc. Sixth International Symposium on Physical Measurement and Signatures in Remote Sensing, 75-83.

Hoppel, W.A., J.W. Fitzgerald, G.M. Frick, R.E. Larson, and E.J. Mack, 1990: Aerosol size distribution and optical properties found in the marine boundary layer over the Atlantic Ocean, *J. Geophys. Res.*, **95,** 95365-95386.

Horvath, H., R.L. Gunter, and S.W. Wilkerson, 1990: Determination of the coarse mode of the atmospheric aerosol using data from a forward scattering spectrometer probe, *Aerosol Sci. Tech.*, **12**, 964-980.

Huebert, B.J., G. Lee, and W.L. Warren, 1990: Airborne aerosol inlet passing efficiency measurement, *J. Geophys. Res.*, **95**, No. D10, 16369-16381.

Kaufman, Y.J., T.W. Brakke, and E. Eloranta, 1986: Field experiment for measurement of the radiative characteristics of a hazy atmosphere, *J. Atmos. Sci.*, **43**, 11, 1135-1151.

Kaufman, Y.J., A. Setzer, D. Ward, D. Tanre, B.N. Holben, P. Menzel, M.C. Pereira, and R. Rasmussen, 1992: Biomass Burning Airborne and Spaceborne Experiment in the Amazonas (BASE-A), *J. Geophys. Res.*, **97,** 14581-14599.

Kaufman, Y.J., A. Gitelson, A. Karnieli, E. Ganor, R.S. Fraser, T. Nakajima, S. Mattoo, and B.N. Holben, 1994: Size distribution and scattering phase function of aerosol particles retrieved from sky brightness measurements, *J. Geophys. Res.*, **99**, No. D5, 10341-10356.

Kaufman, Y.J. and B. Holben, 1996: Hemispherical Backscattering By Biomass Burning and Sulfate Particles Derived for Sky Measurements, *J. Geophys. Res.*, **101,**

Kaufman, Y.J. and D. Tanre, 1997: Algorithm for Remote Sensing of Tropospheric Aerosol from MODIS, EOS Algorithm Technical Background Document, ATBD-MOD-02

Kiehl, J.T. and B.P. Briegleb, 1993: The relative roles of sulfate aerosols and greenhouse gases in climate forcing, *Science*, **260**, 311-314.

Klett, J.D, 1981: Stable analytical inversion solution for processing lidar returns, *Appl. Opt.*, **20**, 211-220.

Liljegren, J.C. and B.M. Lesht, 1997: A Comparison of Integrated Water Vapor from ARM Microwave Radiometes, Radiosondes, and the Global Positioning System at the 1996 Water Vapor IOP, Seventh ARM Science Team Meeting, San Antonio, TX.

Melfi, S.H., R.A. Ferrare, K.D. Evans, B. Demoz, G. Schwemmer, D. Whiteman, D. O'C. Starr, R.G. Ellingson, 1997: Scanning Raman Lidar Measurements of Water Vapor and Aerosols During TARFOX and the Water Vapor IOP, Seventh ARM Science Team Meeting, San Antonio, TX.

Menzel, W.P. and L.E. Gumley, 1997: MODIS Atmospheric Profile Retrieval Algorithm Theoretical Basis Document, EOS Algorithm Technical Background Document, ATBD-MOD-07.

Pilinis, C., S. Pandis, and J. Seinfeld, 1995: Sensitivity of direct climate forcing by atmospheric aerosols to aerosol size and composition, *J. Geophys. Res.*, **100**, No. D9, 18739-18754.

Quinn, P.K., T.L. Anderson, T.S. Bates, R. Dlugi, J. Heintzenberg, W. von Huyningen-Huene, M. Kulmala, P.B. Russell, and E. Swietlicki, 1996: Closure in Tropospheric Aerosol-Climate Research: A Review and Future Needs for Addressing Aerosol Direct Shortwave Radiative Forcing, *Beitr. Phys. Atmosph.*, **69**, No. 4, 547-577.

Ramanthan, V. 1988: The Greenhouse Theory of Climate Change: A Test By an Inadvertent Global Experiment, *Science*, **240**, 293-299.

Remer, L., S. Gasso, D. Hegg, Y. Kaufman, and B. Holben, 1997: Urban/Industrial Aerosol: Ground-Based Sun/Sky Radiometer and Airborne In Situ Measurements, *J. Geophys. Res.*, in press.

Shettle, E.P, 1984: Optical and radiative properties of a desert aerosol model, *Proc. Symposium on Radiation in the Atmosphere*, G. Fiocco, Ed., A. Deepak Publishing, 74-77.

Shettle, E.P. and R.W. Fenn, 1979: Models for the aerosols of the lower atmosphere and the effects of humidity variations on their optical properties, AFGL-TR-79-0214, Air Force Geophysics Laboratory.

Smith, W.L. W.F. Feltz, R.O. Knuteson, and H. E. Revercomb, 1995: PBL Sounding and Cloud Emittance Observations with ARM-CART AERI Observations. *Proceedings of the Fifth Atmospheric Radiation Measurement (ARM) Science Team Meeting.*

Soden, B.J., S.A. Ackerman, D. O'C Starr, S.H. Melfi, and R.A. Ferrare, 1994: Comparison of upper tropospheric water vapor from GOES, Raman lidar, and CLASS measurements during FIRE-II. *J. Geophys. Res.*, *J. Geophys. Res.*, **99,** No. D10, 21005-21016. 1994.

Spinhirne, J.D., D.L. Hlavka, and V.S. Scott, 1996: Aerosol Profiling by Micropulse Lidar at ARM Sites, Second ARM Aerosol Workshop, November, 1996.

Turner, D.D., and J. Goldsmith, 1997: CART Raman Lidar Water Vapor Measurements During the ARM 1996 Water Vapor IOP, Seventh ARM Science Team Meeting, San Antonio, TX.

Wang, J.R., S.H. Melfi, P. Racette, D.N. Whiteman, L.A. Chang, R.A. Ferrare, and K.D. Evans, F.J. Schmidlin , , 1995: Simultaneous Measurements of Atmospheric Water Vapor with MIR, Raman Lidar, and Rawinsondes, *J. Appl. Meteor*, **34**, No. 7, 1595-1607.

# GSFC Scanning Raman Lidar
# Water Vapor Calibration History

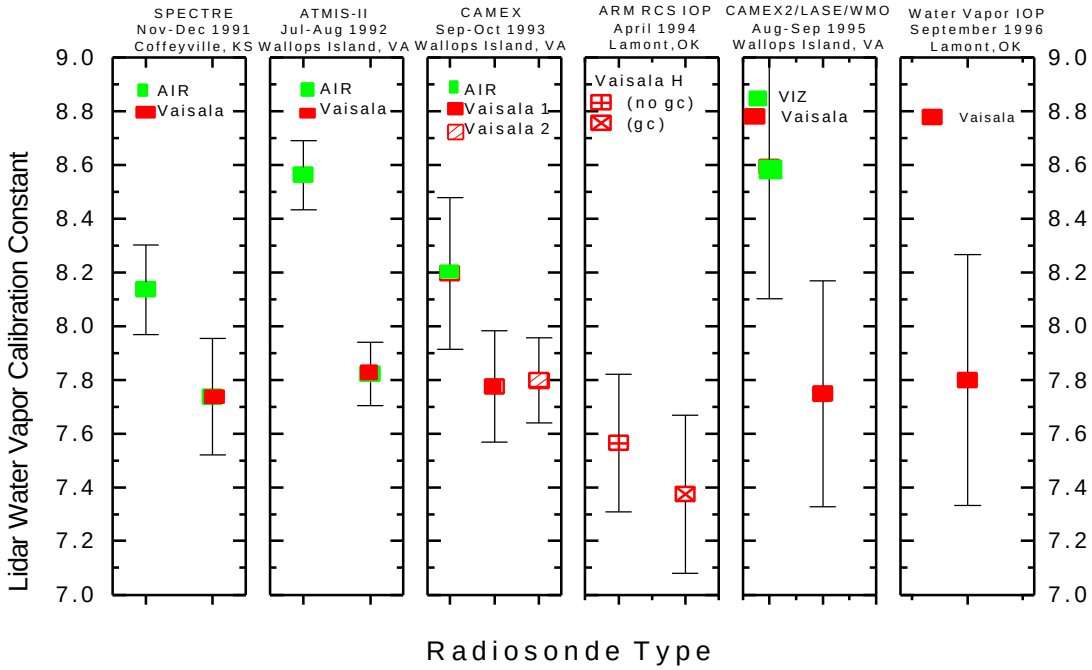


Figure 1. SRL water vapor calibration constant as determined by comparisons with various types of radiosondes.

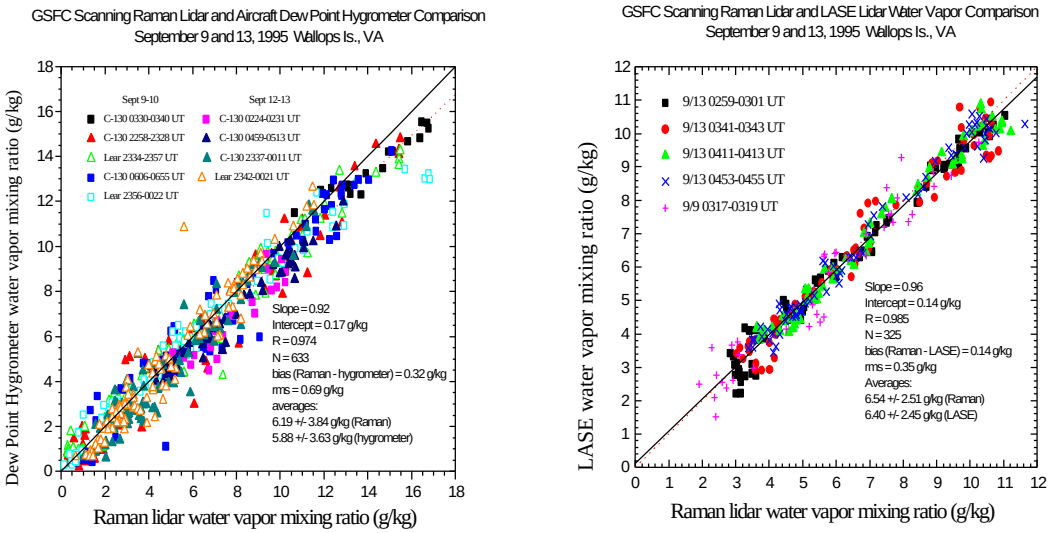


Figure 2. (left) Comparison of dewpoint hygrometer and SRL water vapor mixing ratio measurements acquired during the LASE validation experiment at Wallops Island, VA in September, 1995. (right) Same except for LASE DIAL lidar and SRL water vapor mixing ratio measurements during the same experiment.

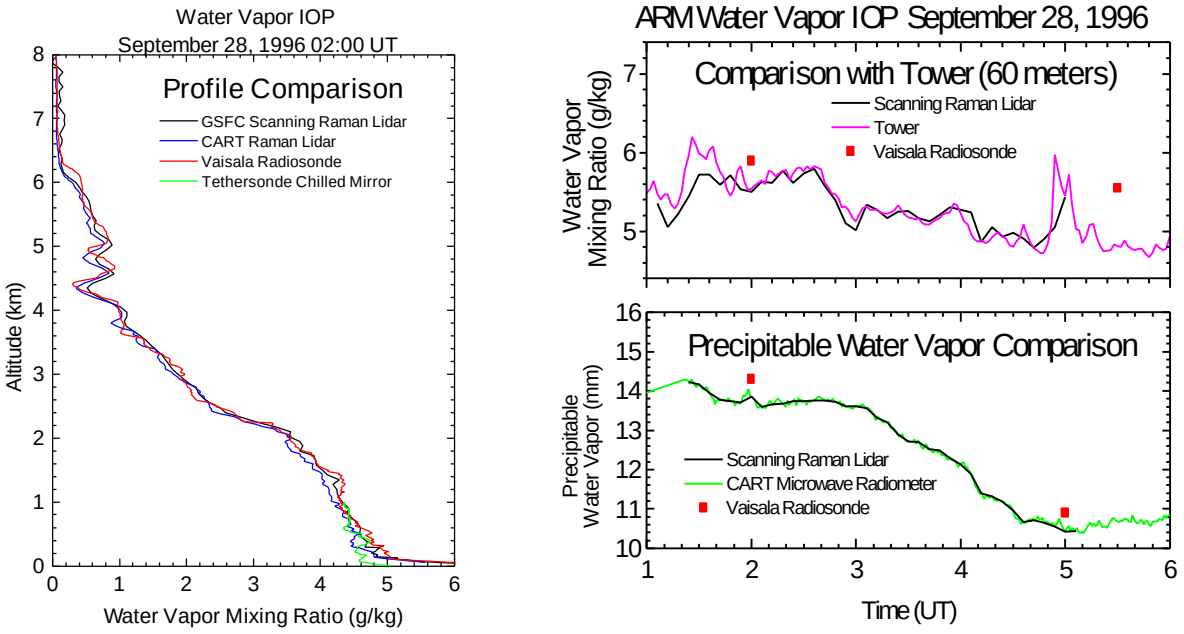


Figure 3. Comparisons of SRL water vapor measurements acquired on September 28, 1996 at the Water Vapor IOP at the DOE SGP site in Oklahoma.

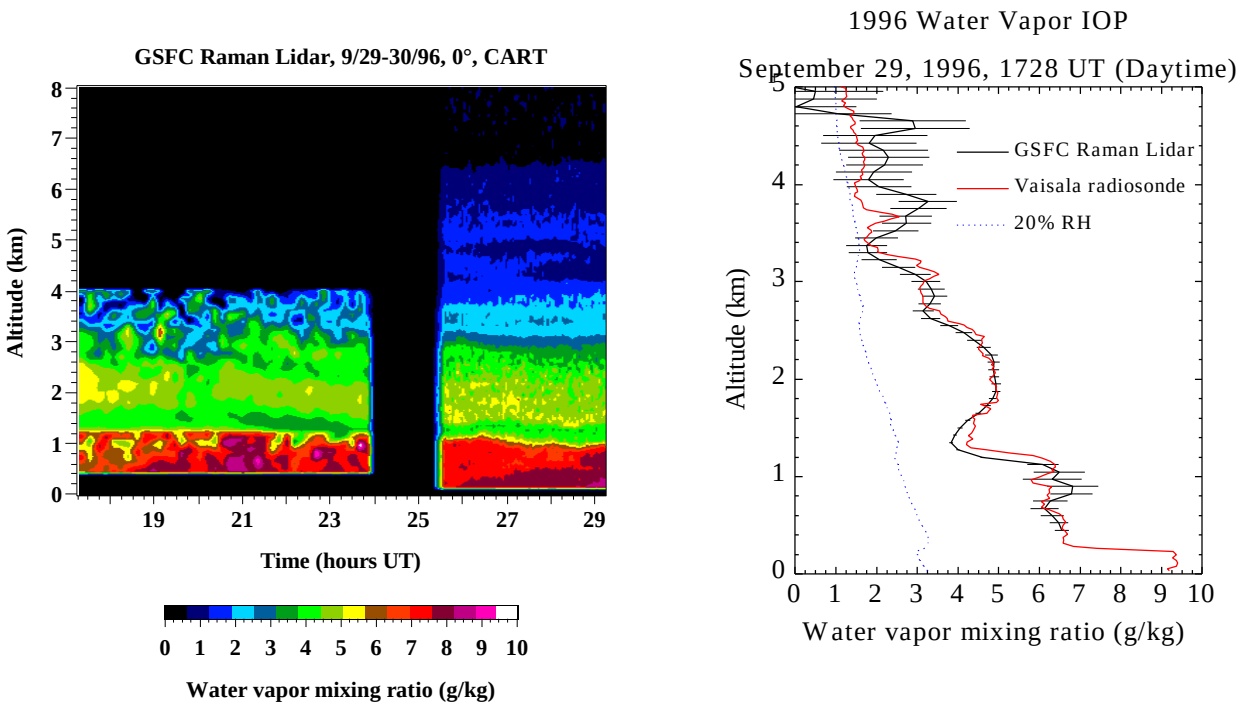


Figure 4. (left) Image showing both daytime and nighttime water vapor measurements acquired by the SRL on September 29, 1996 at the SGP site. ( right) comparison of a SRL daytime water vapor profile with the profile measured by a Vaisala radiosonde.

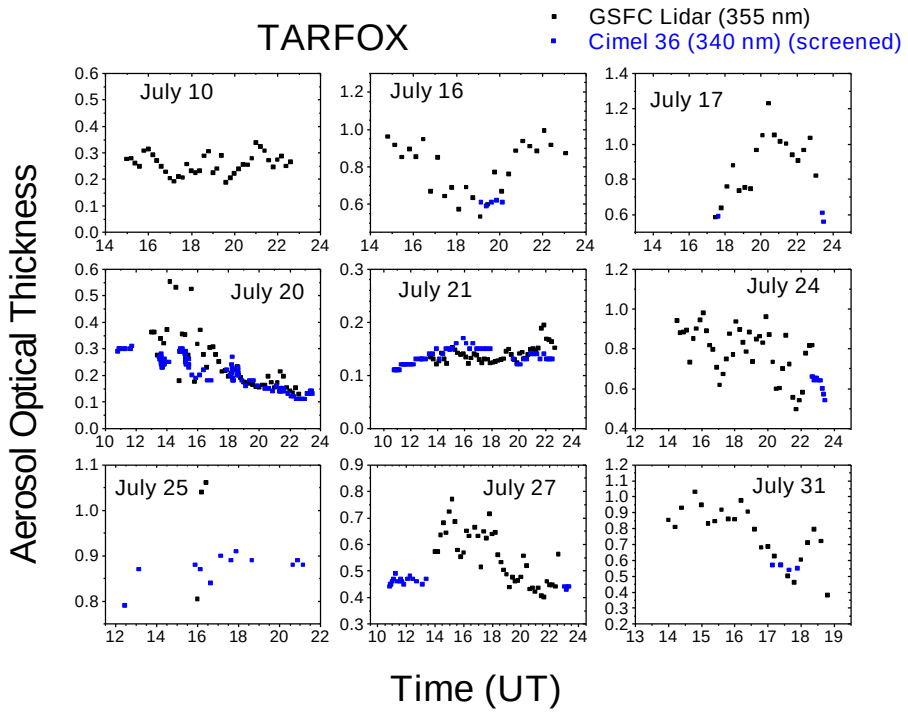


Figure 5. Aerosol optical thickness measured by GSFC Raman lidar and Cimel sun photometer during TARFOX in July, 1996 at Wallops Is.,VA.

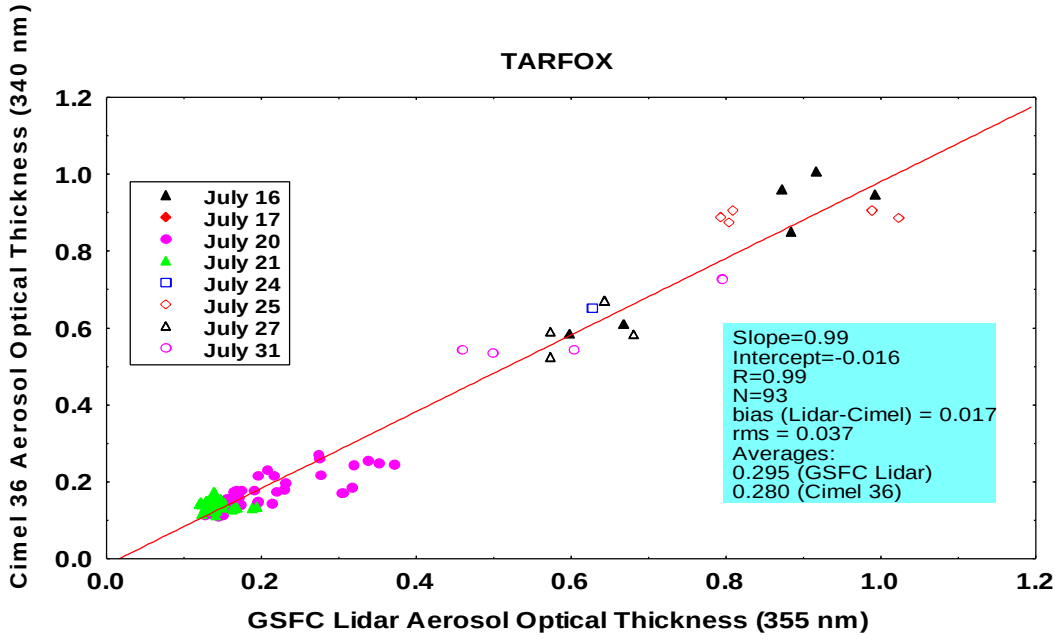


Figure 6. Comparison of the aerosol optical thickness measured by the SRL and Cimel sun photometer during TARFOX in July, 1996 at Wallops Is., VA.

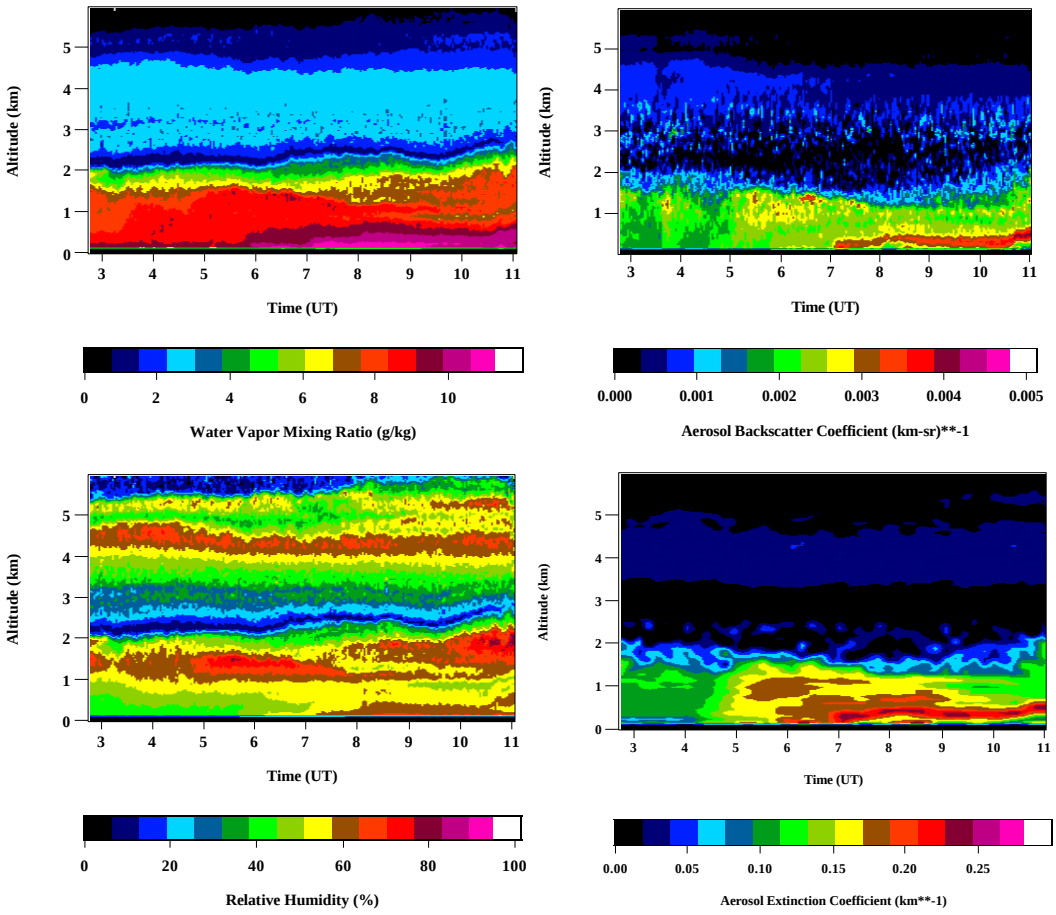


Figure 7. Water vapor mixing ratio (top left), relative humidity (bottom left), aerosol backscattering coefficient (top right), and aerosol extinction coefficient (bottom right) measured by the GSFC Raman Lidar on April 21, 1994 during the RCS IOP.

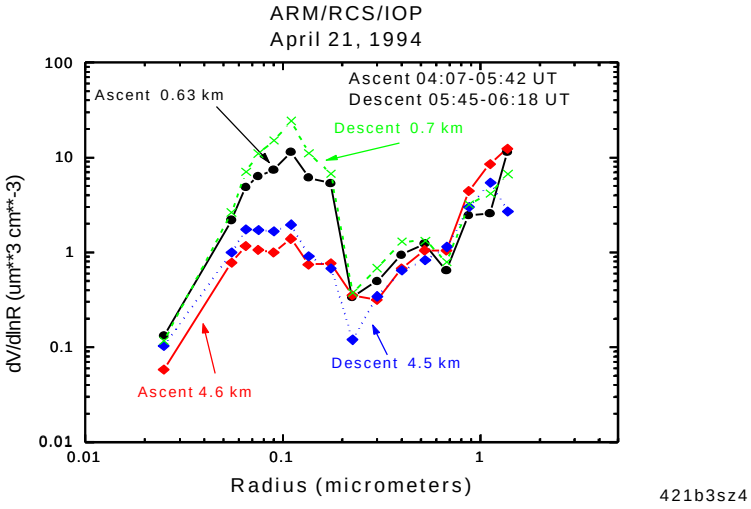


Figure 8. Aerosol volume size distributions measured by the PCASP instrument flown on the UND Citation on April 21, 1994 during the RCS IOP. Aircraft data provided by Mike Poellet (UND).

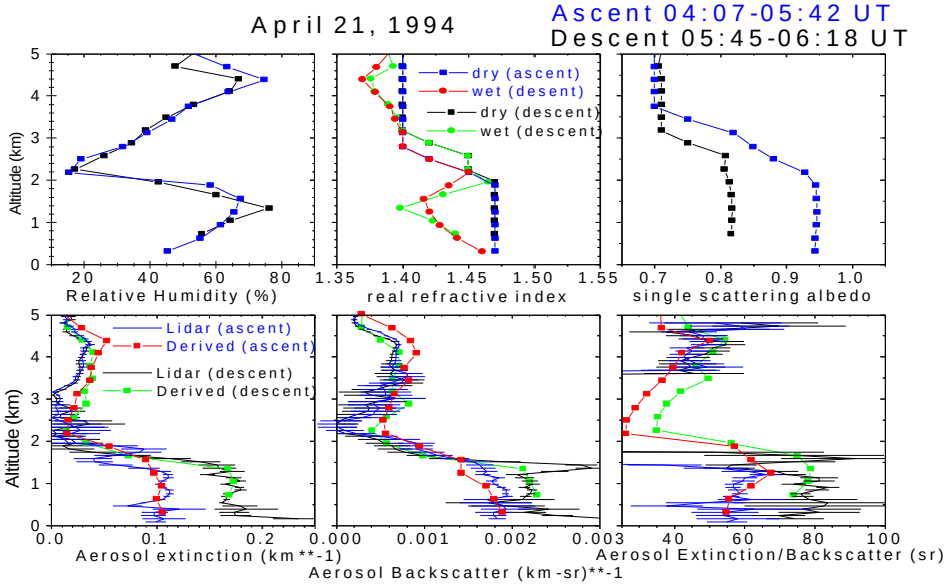


Figure 9. a) (top left) Relative humidity measured by hygrometer during UND Citation flight on the night of April 21, 1994. b) ( top middle) dry and wet real refractive indices computed for aerosol extinction and backscattering profiles derived using PCASP aerosol size distributions. c) (top right) derived single scattering albedos d) (bottom left) aerosol extinction coefficient, e) (bottom middle) aerosol backscattering coefficient, and f) (bottom right) aerosol extinction/ backscattering ratio measured by the lidar and derived from the aerosol size distribution measured by the PCASP instrument.

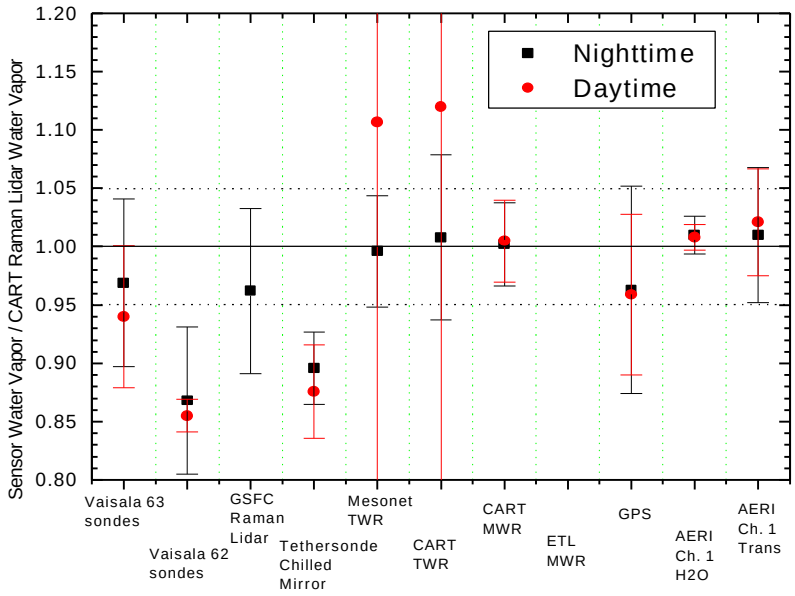


Figure 10. Comparison of CART Raman Lidar water vapor measurements with those acquired by other sensors during the Water Vapor IOP held in September, 1996.

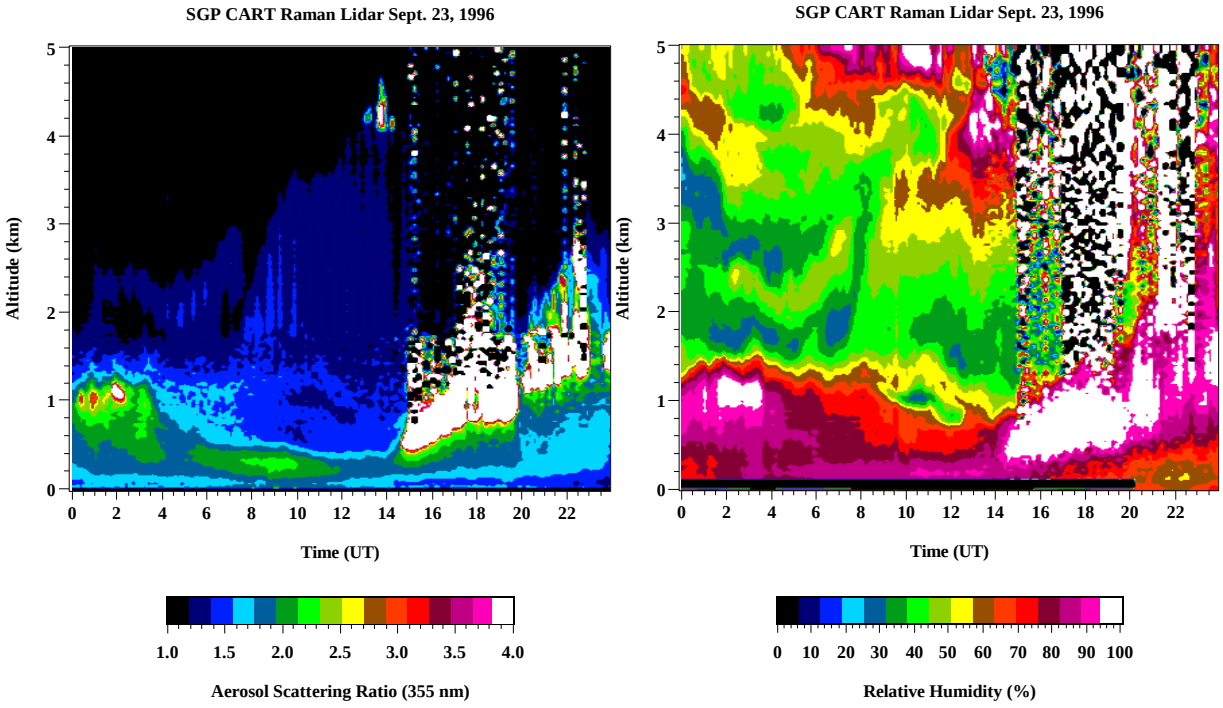


Figure 11. (left) Aerosol scattering ratio measured by the SGP CART Raman Lidar on September 23, 1996 during the Water Vapor IOP. ( right) Relative humidity derived from SGP CART Raman Lidar measurements of water vapor mixing ratio and temperature profiles derived from AERI radiances.